Journal of Power Sources 214 (2012) 1–6

Contents lists available at SciVerse ScienceDirect

Journal of Power Sources

journal homepage: www.elsevier.com/locate/jpowsour

Structure and electrochemistry of scaling nano C–$LiFePO_4$ synthesized by hydrothermal route: Complexing agent effect

F. Brochu [a], A. Guerfi [a], J. Trottier [a], M. Kopeć [b,c], A. Mauger [b], H. Groult [d], C.M. Julien [d], K. Zaghib [a,*]

[a] Institut de Recherche d'Hydro-Québec, 1800 Bd Lionel-Boulet, Varennes, Québec, Canada J3X 1S1
[b] Université Pierre et Marie Curie – Paris 6, Institut de Minéralogie et de Physique des Milieux Condensée, 140 rue de Lourmel, 75015 Paris, France
[c] Warsaw University of Technology, Warszawa, Poland
[d] Université Pierre et Marie Curie – Paris 6, PECSA, UMR 7195, 4 place Jussieu, 75005 Paris, France

ARTICLE INFO

Article history:
Received 16 February 2012
Received in revised form
26 March 2012
Accepted 29 March 2012
Available online 24 April 2012

Keywords:
Olivine
Hydrothermal synthesis
Chelating agent
Cathode materials
Li-ion batteries

ABSTRACT

Submicronic particles of $LiFePO_4$ were synthesized by hydrothermal method at 185 °C assisted by carboxylic acid route. In this work, we used citric acid to control the pH of the final products and studied the influence of synthetic conditions on the physical and electrochemical properties of $LiFePO_4$. Structural characterization includes XRD, SEM, TEM and FTIR experiments. The powder quality was investigated by magnetic measurements. Electrochemical features of C–$LiFePO_4$ in Li cell using 1 mol L^{-1} $LiPF_6$-EC-DEC electrolyte show an excellent capacity retention of 158 mAh g^{-1} for material prepared with *R*(citric acid/Fe) = 7 mol%.

1. Introduction

$LiFePO_4$ (LFP) is now considered as active cathode materials in the new generation of Li-ion batteries. After the pioneering work of Padhi *et al.* [1], the problem of the low intrinsic electrical conductivity has been solved by coating the particles by conductive carbon [2]. Then, the preparation of the material has been improved to remove the impurities that poisoned the electrochemical performance [3]. Nowadays, many different synthesis routes can be used to prepare $LiFePO_4$ of good quality, which have been reviewed recently [4], and $LiFePO_4$ is now available on the market exhibiting capacity retention close to its theoretical one (170 mAh g^{-1}). However, the growing demand of the product justifies efforts to optimize the synthesis in terms of price and electrochemical performance. Two main synthesis approaches are used today on the tonnage quantities. One is the solid-tate reaction, which is a synthesis route at high temperature the order of 700 °C, including the synthesis from the molten state [5] that has been proposed as an option to reduce the price. The other one is the hydrothermal/solvothermal approach, particularly successful with respect to controlling the chemical composition and crystallite size [6–9]. The conventional hydrothermal process involves a reaction time 5–12 h to synthesize $LiFePO_4$ [10–18]. With respect to the previous techniques, the hydrothermal process has the advantage that the synthesis temperature can be as small as 180 °C [19], so that it is a low energy consuming synthesis process. In these earlier works, the synthesis was assisted by ascorbic acid. On another hand, we have already mentioned the need for coating the particles with conductive carbon. This is easy and almost free in synthesis at elevated temperature, since it is sufficient to add a carbon precursor, typically lactose, to the precursors of $LiFePO_4$ so that the synthesis of carbon-coated particles is a one-step process. However, the carbon deposit is conductive only when the carbonization temperature is $T_{ca} \geq 600$ °C [20–22]. In that case, the carbon layer is typically coke, a conductive variety of carbon [22]. On another hand, at lower values of T_{ca}, the formation of sp^3 bonds at the expense of sp^2 is detrimental to the conductivity. To face this problem in case of hydrothermal synthesis, two options have been considered. One is to add conductive carbon under the form of carbon nanotubes in the autoclave [19], but nanotubes are very expensive. The other one is to add an additional step to the synthesis, using hydrothermal synthesis as the formation step for preparing LiFePO4, which material subsequently undergoes a high-temperature carbon coating step. In that case, the high-priced

* Corresponding author. Tel.: +1 450 652 8019; fax: +1 450 652 8424.
E-mail address: zaghib.karim@ireq.ca (K. Zaghib).

0378-7753/$ – see front matter © 2012 Elsevier B.V. All rights reserved.
doi:10.1016/j.jpowsour.2012.03.092

carbon nanotubes are avoided, but the advantage of the low-temperature synthesis in terms of energy consumption is lost. So far, only this second process has been adopted at the industrial scale, by Sud-Chimie [23,24].

In this work, we have synthesized submicron-sized $LiFePO_4$ materials using the hydrothermal route assisted by a carboxylic acid, namely the citric acid, instead of the ascorbic acid used in the literature. Various synthesis parameters have been considered, including molar stoichiometry and pH of the starting solution. The structural characterization has been achieved by XRD, SEM, TEM, FTIR and magnetic measurements. To investigate electrochemical properties as a function of the synthesis conditions, the lactose route [25] has been used as the additional carbon-coating step, like in the industrial process. We find that the pH of the solution used for the preparation is critical to the electrochemical properties. Excellent results are obtained for the citric acid/Fe ratio $R = 7$ mol%, otherwise, the incomplete reduction of iron results in the formation of γ-Fe_2O_3 impurities that reduce importantly the capacity.

2. Experimental

2.1. Synthesis

Submicron-sized powders were prepared by hydrothermal route assisted by complexing agent as shown in Fig. 1. We used $FeSO_4 \cdot 7H_2O$, H_3PO_4 and $LiOH \cdot H_2O$ as chemical precursors. Attention has been taken to choose the proportion of the precursors corresponding to stoichiometry. 30 mL of solution was introduced in the Parr bomb 50 mL in volume. We have investigated elsewhere the consequence of a departure from stoichiometry [26]. The Li deficiency in the preparation process results in a partial occupation of Li sites by Fe, forming the defect $Fe^{\bullet}_{Li} + V'_{Li}$ in the Kröker–Vink notation. Therefore, the chemical formula switches to $Li_{1-2x}Fe_xFePO_4$ or, in closed form, $Li_{1-2x}Fe_{1+x}PO_4$ [26]. This defect has also been observed in samples synthesized by hydrothermal at temperature below 200 °C [6,19]. At concentration $x > 3\%$, this defect precipitates under the form of sarcopside, $Fe_3(PO_4)_2$ [26], which may be the reason why mineralogists have observed sarcopside and triphylite associations in pegmatites [27]. The $Fe^{\bullet}_{Li} + V'_{Li}$ defect has dramatic effects on the electrochemical properties since it blocks the Li-channel where it is located. To the opposite, an excess of Li in the preparation process results in the formation of Li_3PO_4 at the surface of the $LiFePO_4$ particles [26]. The consequences on the electrochemical properties are much less dramatic since the Li-channels remain open, but still the impurity is an inert mass that reduces the capacity.

After pH control by adjusting the acid/Fe ratio, the aqueous solution was heated at 185 °C in Teflon-type autoclave for few hours. The wetted powder was dried for 2 h in controlled atmosphere (argon). Optimized nanosized particles, elongated shape were obtained with the ratio acid/Fe = 7 mol%. The results are thus reported here for samples prepared with this acid/Fe ratio, and for samples without any complexing agent for comparison. The corresponding pH without complexing agent measured in the initial product (step 1 in Fig. 1) is 8.23, and 3.57 in the wetted powder (step 3). In the case of acid/Fe = 7 mol%, the pH values are 6.47 and 3.67, respectively.

The carbon coating was achieved using the procedure described elsewhere [25]: the particles were mixed with the carbon precursor (lactose) in acetone solution. The nominal dry additive corresponded to 5 wt% carbon in $LiFePO_4$. After drying, the blend was heated at 650 °C for 2 h in an inert atmosphere. The final quantity of carbon was about 2 wt% of the material (Cdetector, LECO Co., CS 444). This process leads to a homogeneous, 3 nm-thick surface layer of conductive carbon [25].

2.2. Apparatus

Structural analysis of the samples were characterized with X-ray diffraction (XRD) on a Philips X'Pert PRO MRD (PW3050) diffractometer equipped with a Cu anticathode (CuKα radiation $\lambda = 1.54056$ Å) at room temperature. XRD patterns were collected under Bragg–Brentano geometry at 2θ with step 0.025° in the range 10–80°. For morphological analysis, a scanning electron microscope (SEM) study of the samples was performed using a Hitachi (Japan) electron microscope. The magnetic measurements (susceptibility and magnetization) were performed with two fully automated SQUID magnetometer (Quantum Design MPMS-5S) in the temperature range 4–300 K as described elsewhere [3].

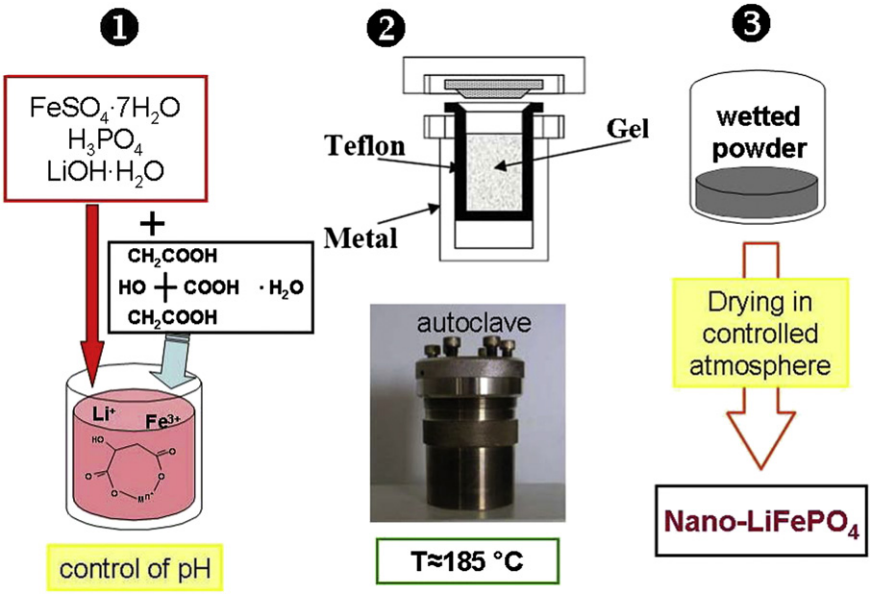

Fig. 1. Flowchart of the hydrothermal method before carbon-coating.

2.3. Electrochemistry

The electrochemical properties were tested at room temperature in cells with metallic lithium as anode electrode. Charge–discharge tests were performed on coin type cell (CR2032). Composite positive electrode was prepared by thoroughly mixing the active material (90 wt%) with vapor grown carbon fiber (2 wt%), acetylene black (2 wt%), polyvinylidene fluoride (6 wt%) in N-methyl-pyrrolidinone and spread onto aluminum foils then dried for 24 h at 120 °C in vacuum. Cathode loading was 9 mg/cm^2. Cells were then assembled in an argon-filled glove box using foils of Li metal as counter electrode and Celgard 2400 as separator. The electrolyte was 1.0 mol L^{-1} $LiPF_6$ in a mixture of ethylene carbonate (EC) and diethyl carbonate (DEC) (1:1, v/v). The cells were galvanostatically cycled between 2.0 and 4.0 V *vs.* Li^0/Li^+ on a Mac-Pile battery cycler at room temperature.

3. Results and discussion

Fig. 2 shows the X-ray diffraction patterns and the Rietveld refinements of the LFP samples prepared without chelating agent and with citric acid/Fe $R = 7$ mol%. All the diffraction lines can be indexed in the orthorhombic system with the *Pnma* space group. No impurity has been detected in these spectra. However, we shall see hereunder that the much more sensitive magnetic measurements will reveal the presence of some impurities in case the samples are prepared without chelating agent. Parameters of Rietveld refinement for the stoichiometric LFP sample prepared with chelating agent citric acid ($R = 7$ mol%) and without chelating agent are reported in Tables 1 and 2, respectively.

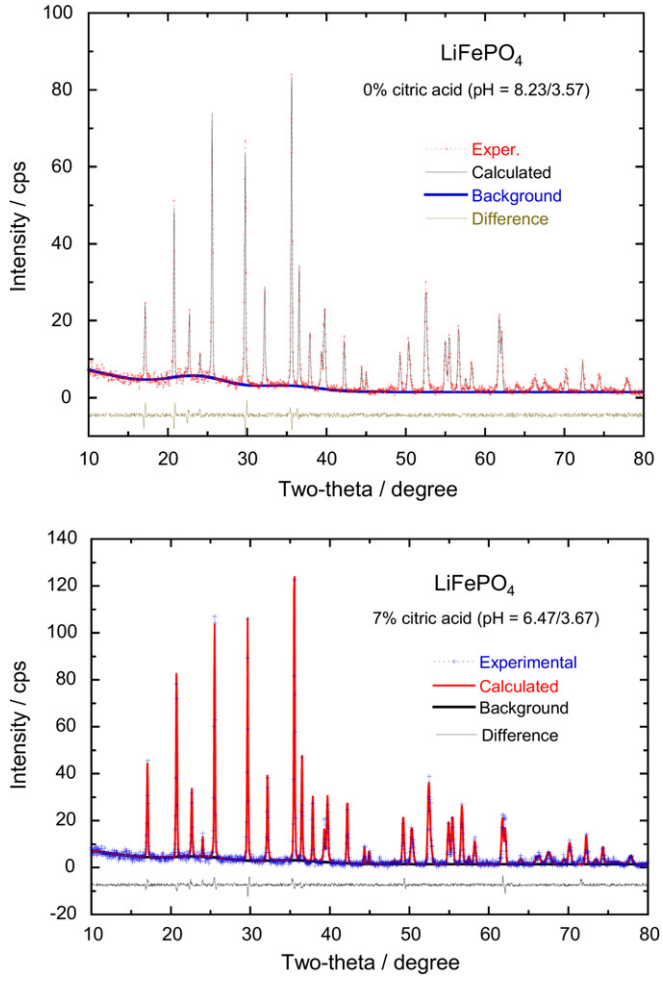

Fig. 2. XRD patterns and Rietveld refinements of $LiFePO_4$ powders prepared without any chelating agent (upper spectrum) and with citric acid as chelating agent (lower spectrum). The corresponding pH at the first and third steps of the synthesis (see Fig. 1) are indicated in the figures.

Table 1
Results of Rietveld refinement for the stoichiometric LFP sample prepared with chelating agent citric acid/Fe $R = 7$ mol%.

Site	Wyck.	*x*	*y*	*z*	Atom	Occ	Beq
Li1	4*a*	0	0	0	Li^{+1}	0.9967(31)	1
					Fe^{+2}	0.0033(31)	1.32(2)
Fe1	4*c*	0.2823(7)	0.25	0.9741(9)	Fe^{+2}	1	1.32(2)
P1	4*c*	0.0946(3)	0.25	0.4170(13)	P	1	1.30(1)
O1	4*c*	0.0980(8)	0.25	0.7446(16)	O^{-2}	1	1.46(1)
O2	4*c*	0.4529(9)	0.25	0.2083(15)	O^{-2}	1	1.46(1)
O3	8*d*	0.1663(9)	0.0437(5)	0.2826(9)	O^{-2}	1	1.46(1)

R-Bragg = 2.173.
Phase $LiFePO_4$, space group *Pnma*(62).
$a = 10.3243(1)$ Å, $b = 6.0062(2)$ Å, $c = 4.6926(1)$ Å, $V = 290.98(7)$ Å^3.

The refined lattice parameters of the LFP sample with chelating agent are $a = 10.3243(1)$ Å, $b = 6.0062(2)$ Å, $c = 4.6926(1)$ Å, and $V = 290.98(7)$ Å^3; all of them are in good agreement with the values reported in the literature [28,29]. The average mono-crystallite size was calculated from the XRD line width using the Scherrer's formula, $d = 0.9\lambda/\beta_{1/2}\cos\theta$, where λ is the X-ray wavelength, $\beta_{1/2}$ is the corrected width at half-height of the main diffraction peaks, and θ is the diffraction angle. The procedure to determine $\beta_{1/2}$ has been reported elsewhere [30]. The parameter d has been measured for different angles corresponding to the (200), (101), (111), (211) and (311) lines. No significant dependence on θ has been evidenced, and the result is $d = 55 \pm 5$ nm.

The lattice parameters of the sample prepared without chelating agent are $a = 10.3298(2)$ Å, $b = 6.0097(8)$ Å, and $c = 4.693(1)$ Å. The volume of the unit cell is then $V = 291.3(3)$ Å^3. This volume is significantly different from that of stoichiometric $LiFePO_4$, and gives evidence of the presence of $Fe^{\bullet}_{Li} + V'_{Li}$ defect. We have investigated elsewhere the linear variation of the volume of the unit cell with the concentration of this defect [26]. From this relation, we can estimate the concentration of such defects to 4.6%.

The morphology of LFP powders is depicted by the SEM images shown in Fig. 3. SEM images show clearly the influence of the complexing agent. The material synthesized without the chelating agent is made of particles that appear as thick tiles with a broad dispersion in size. On another hand, the particles obtained in presence of the chelating agent have a more regular shape, about 240 nm-thick and 1 μm-length, and the size dispersion is narrow.

The local structure was investigated by FTIR spectroscopy (Fig. 4). The spectrum of $LiFePO_4$ has been already reported and

Table 2
Results of Rietveld refinement for the Li-defective LFP sample prepared without chelating agent.

Site	Wyck.	*x*	*y*	*z*	Atom	Occ	Beq
Li1	4*a*	0	0	0	Li^{+1}	0.9329(2)	1
					Fe^{+2}	0.0461(2)	1.25(5)
Fe1	4*c*	0.2823(15)	0.25	0.9731(22)	Fe^{+2}	1	1.25(5)
P1	4*c*	0.0935(21)	0.25	0.4168(22)	P	1	1.75(7)
O1	4*c*	0.1000(13)	0.25	0.7475(13)	O^{-2}	1	1.32 (8)
O2	4*c*	0.4548(11)	0.25	0.2081(11)	O^{-2}	1	1.32(8)
O3	8*d*	0.1681(8)	0.0431(9)	0.2824(9)	O^{-2}	1	1.32(8)

R-Bragg = 2.238.
Phase $LiFePO_4$, space group *Pnma*(62).
$a = 10.32980(2)$ Å, $b = 6.00971(8)$ Å, and $c = 4.6931(1)$ Å, $V = 291.32(3)$ Å^3.

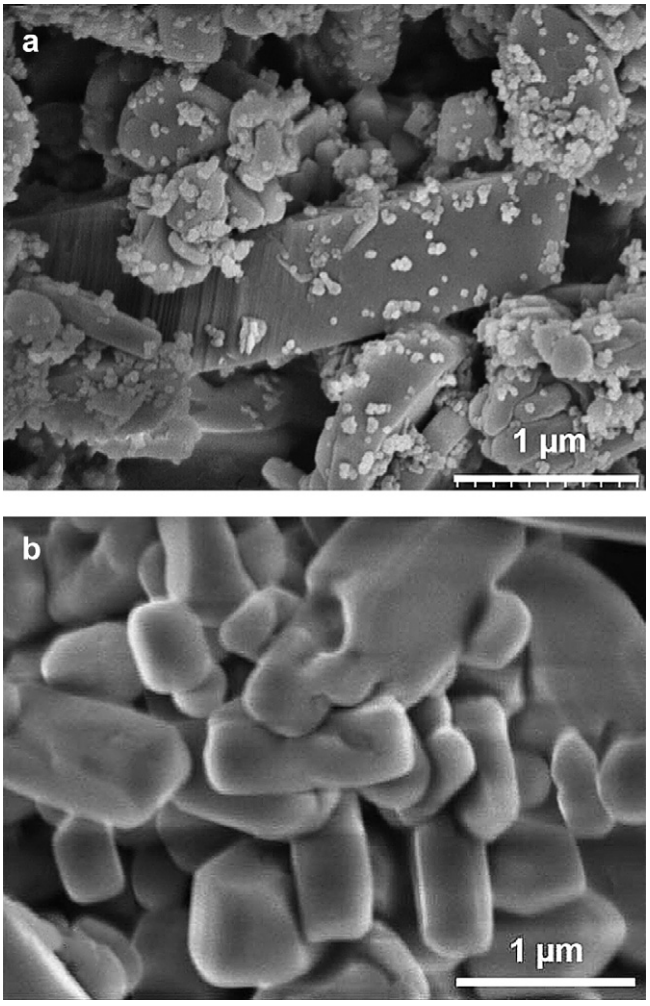

Fig. 3. SEM images of hydrothermal LFP powders synthesized without complexing agent (left) and with citric acid/Fe $R = 7$ mol% (right).

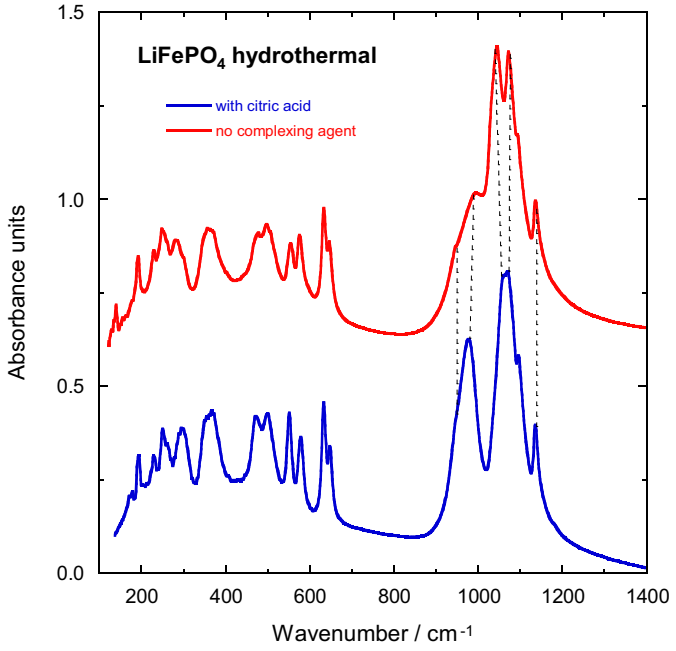

Fig. 4. FTIR spectra of LFP powders synthesized by hydrothermal route.

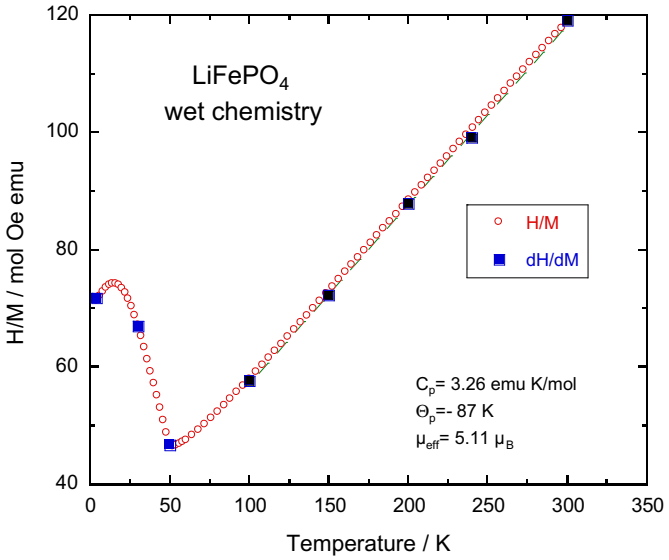

Fig. 5. Magnetization curves of the sample synthesized with citric acid/Fe $R = 7$ mol%.

analyzed elsewhere [31,32]. The spectrum of the sample with $R = 7$ mol% is characteristic of well-crystallized $LiFePO_4$ [33]. Again, we detect significant modification due to the influence of the weak acid used for the hydrothermal synthesis. The broadening of the bands in the spectra of the sample without chelating agent gives evidence of the shorter lifetime of the lattice vibrations, and thus a lattice disorder in this sample. That is true for the low-frequency modes to which Li is associated, but also for the dominant bands in the range 900–1200 cm^{-1}, which is the region of the asymmetric and symmetric stretching modes of PO_4^{3-} structural units. This result is then constant with the analysis of the XRD spectra. The disorder revealed by the FTIR spectrum of the sample synthesized in absence of the chelating agent is another evidence of the $Fe^{\bullet}_{Li} + V'_{Li}$ defects. The positive charge on $Fe^{\bullet}_{Li}$ and the negative charge on V'_{Li} generate electrostatic fields that compensate at distance significantly larger than the lattice parameter, but not at the molecular scale probed by the FTIR, so that the FTIR experiments are quite sensitive to this defect.

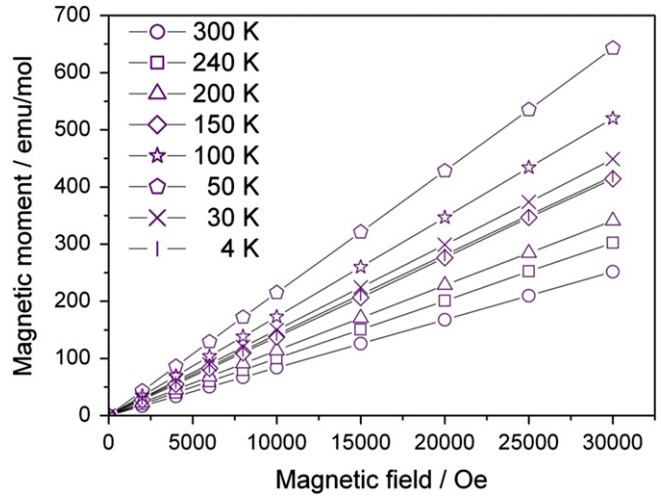

Fig. 6. Reciprocal magnetic susceptibility of $LiFePO_4$ nano-powder. The phase purity is shown by the coincidence of the H/M and dH/dM data points. Also, the magnetic moment $\mu = 5.11\ \mu_B$ is close to the theoretical one (4.9 μ_B).

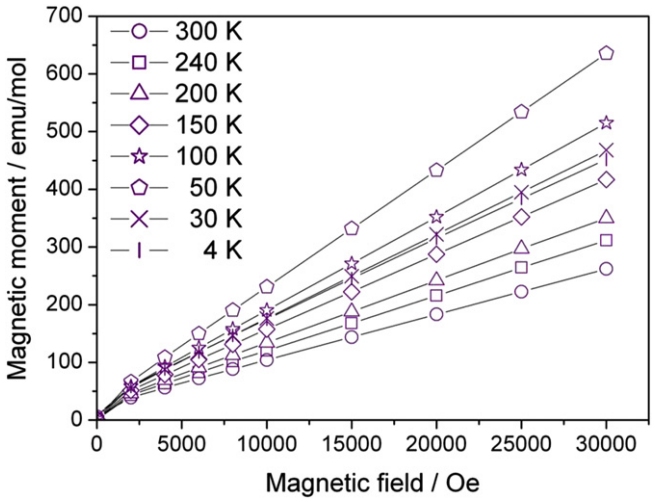

Fig. 7. Reciprocal magnetic susceptibility of $LiFePO_4$ nano-powder synthesized without complexing agent. The signal decomposes in an extrinsic component that saturates at small magnetic field originating form the meghamite impurity, plus the intrinsic part.

Note, however, that all the bands can be identified as intrinsic bands of $LiFePO_4$, which confirms the absence of any impurity phase in the bulk of the particles. This is at contrast with the impurities that have been detected on FTIR spectra of samples prepared by other synthesis routes below 400 °C [34].

SQUID magnetometer experiments are very sensitive to even small (less than 1%) amount of impurities [3]. The magnetization curves $M(H)$ for the sample grown with $R = 7$ mol% is reported in Fig. 6 and is linear in field. The temperature dependence of susceptibility $\chi = M/H$ at magnetic field $H = 10$ kOe recorded upon heating the sample from 4.2 K is shown in Fig. 5. The $\chi^{-1}(T)$ curve has been reported instead of $\chi(T)$ to show that the Curie–Weiss law $\chi^{-1}(T) = C/(T + \theta)$ is satisfied in the paramagnetic regime, *i.e.* at temperature larger than the Néel temperature $T_N = 52$ K [35]. The effective magnetic momentum deduced from the Curie constant is $\mu_{eff} = 5.11\ \mu_B$ close to the theoretical value 4.9 μ_B. These data are characteristics of $LiFePO_4$ free from any impurity [36]. On the other hand, the magnetization curves of the sample prepared without the citric acid are non linear, as shown in Fig. 7. These magnetization curves are characteristics of the presence of ferrimagnetic impurities (meghamite γ-Fe_2O_3) in concentration (circa 0.2 at.%) too small to be detected by XRD analysis. Therefore, the citric acid is a reducing agent that prevents the formation of this Fe^{3+}-impurity.

After carbon coating using the lactose route, electrochemical properties have been investigated as a function of the synthetic conditions (Fig. 8). The tests were carried out at C/8 rate in the potential range between 2.0 and 4.0 V *vs.* Li^0/Li^+. Smaller capacity retention is obtained for sample prepared without complexing agent, 140 mAh g^{-1} *vs.* 158 mAh g^{-1} at the second cycle for sample synthesized with $R = 0.07$ mol%. The residual concentration of meghamite impurity cannot explain this 14% decrease in capacity. This decrease is attributable to the $Fe^{\bullet}_{Li} + V'_{Li}$. Although the concentration of this defect is only 0.046 at.%, the impact on the capacity retention is quite significant. This is due to the one-dimensional character of the ionic transport in this material, the

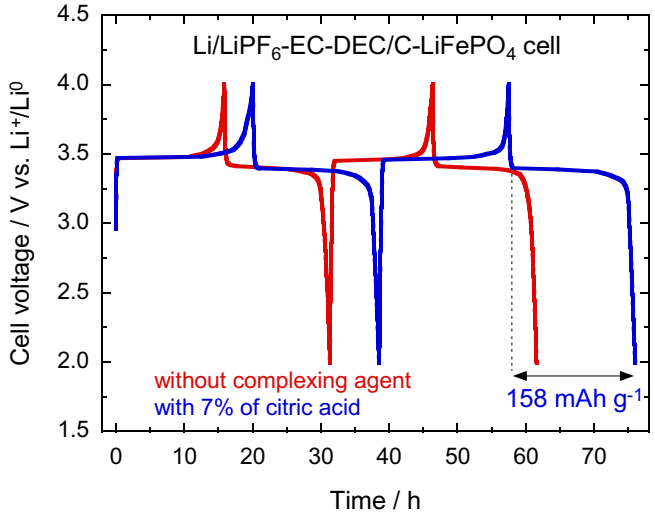

Fig. 8. Charge–discharge profiles of $LiFePO_4$ powders synthesized by hydrothermal route as a function of the complexing agent.

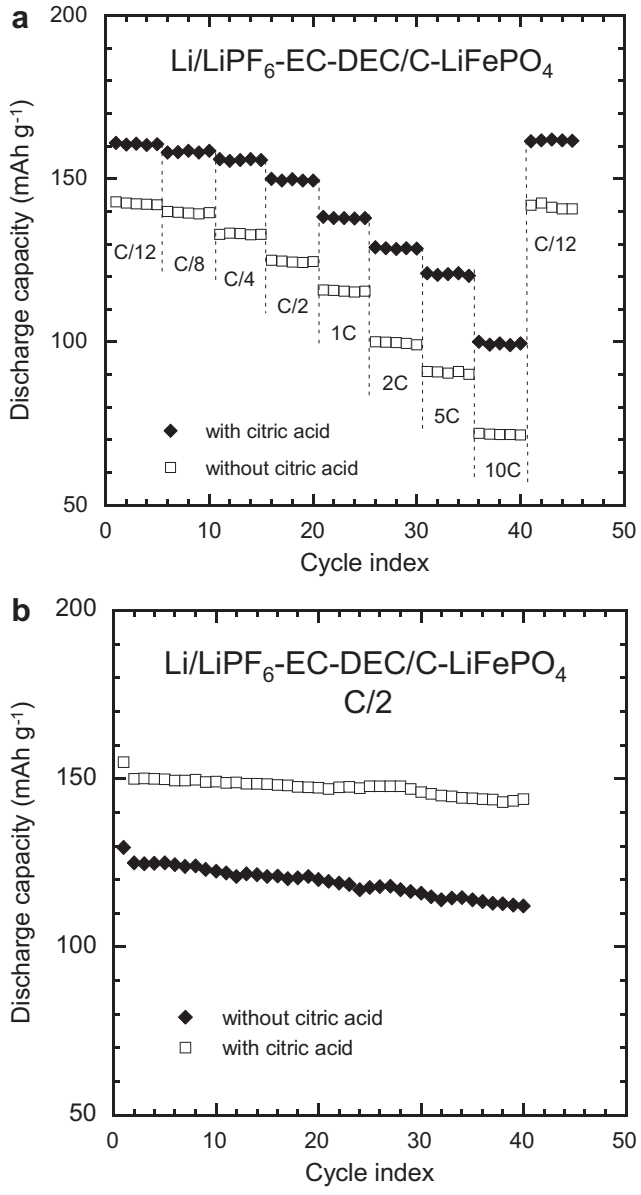

Fig. 9. The electrochemical performance of the LFP samples as a function of the synthetic conditions: (a) The discharge capacity at various C-rates and (b) The discharge capacity *vs.* cycle index at C/2 rate.

iron ion on the Li-site blocking the whole Li-channel where it is located. Fig. 9 displays the electrochemical performance of the LFP samples as a function of the synthetic conditions: the discharge capacity at various C-rates and the discharge capacity *vs*. cycle index at C/2 rate. The discharge capacities at discharge C-rate from C/12 to 10 C are illustrated in Fig. 9a. It is observed that the sample prepared with citric acid possesses the highest capacity at any discharge rates, reaching 100 mAh g^{-1} at 10C compared to 72 mAh g^{-1} for LFP powders synthesized without complexing agent. Note that care was taken to use the same loading (3.1 mg cm^{-2}) for both types of electrodes. The good capacity retention of the LPF powders synthesized with the help of citric acid is attributed to several factors: (i) the effect of nanosized particle and the thickness of the electrode coating about 25 μm (1.55 g cm^{-3} packing density), (ii) the purities of the LFP element as the citric acid acts an efficient reducing agent that prevents Fe^{3+}-based impurities and (iii) the absence of high concentration of $Fe^{\bullet}_{Li} + V'_{Li}$ defects that severely damage the capacity retention of the cathode material. Similarly, the good electrochemical performance of the electrode material synthesized with citric acid is shown in Fig. 9b, which represents the evolution of the discharge capacity against cycling index. Finally, we estimate the volumetric energy density 558 Wh L^{-1} of such an $LiFePO_4$ electrode, assuming 3.0 V the plateau potential at 5C discharge rate.

4. Conclusion

$LiFePO_4$ has been successfully grown using hydrothermal method assisted by citric acid. Optimized nano-particles are obtained for acid/Fe ratio of 7 mol%. For such synthesis particles are free of any ferromagnetic impurities such as meghamite. Citric acid has two functions: (i) It acts as a reducing agent that prevents the formation of Fe^{3+} impurities. (ii) It favors the crystallization at low temperature as it prevents the formation of $Fe^{\bullet}_{Li} + V'_{Li}$ defects that are severely damaging the capacity retention of this cathode element. This is actually a non-trivial effect since iron remains divalent in this defect. Therefore the presence of this defect not only depends on the synthesis temperature used in the hydrothermal process, but also on the nature of the chelating agent, and the results shows that the carboxylic acid is very efficient to eliminate it. $LiFePO_4$ grown by hydrothermal route at 185 °C with citric acid/Fe ratio of 7 mol% exhibits remarkable capacity retention ~158 mAh g^{-1} (at the 2nd cycle).

References

[1] A.K. Padhi, K.S. Nanjundaswamy, J.B. Goodenough, J. Electrochem. Soc. 144 (1997) 1188.
[2] N. Ravet, Y. Chouinard, J.F. Magnan, S. Besner, M. Gauthier, M. Armand, J. Power Sources 144 (2001) 1188.
[3] A. Ait-Salah, A. Mauger, C.M. Julien, F. Gendron, Mater. Sci. Eng. B 129 (2006).
[4] C.M. Julien, A. Mauger, K. Zaghib, J. Mat. Chem. 21 (2011) 9955.
[5] K. Zaghib, P. Charest, M. Dontigny, A. Guerfy, M. Lagacé, A. Mauger, M. Kopek, C.M. Julien, J. Power Sources 195 (2010) 8280.
[6] J. Chen, M.S. Whittingham, Electrochem. Commun. 8 (2006) 855.
[7] S. Yang, P.Y. Zavajil, M.S. Whittingham, Electrochem. Commun. 3 (2001) 505.
[8] K. Dokko, S. Koizumi, K. Kanamura, Chem. Lett. 35 (2006) 338.
[9] A.V. Murugan, T. Muraliganth, A. Manthiram, J. Electrochem. Soc. 156 (2009) A79.
[10] G. Meligrana, C. Gerbaldi, N. Penazzi, J. Power Sources 160 (2006) 516.
[11] K. Shiraishi, K. Dokko, K. Kanamura, J. Power Sources 146 (2005) 555.
[12] S. Franger, F. Le Cras, C. Bourbon, H. Rouanlt, J. Power Sources 119–121 (2003) 252.
[13] S. Tajimi, Y. Ikeda, K. Uematsu, K. Toda, M. Sato, Solid State Ionics 175 (2004) 287.
[14] J. Lee, A.S. Teja, Mater. Lett. 60 (2006) 2105.
[15] K. Dokko, S. Koizumi, K. Sharaishi, K. Kananura, J. Power Sources 165 (2007) 656.
[16] B. Jin, H.-B. Gu, Solid State Ionics 178 (2008) 1907.
[17] E.M. Jin, B. Jin, D.-K. Jun, K.-H. Park, H.-B. Gu, K.-W. Kim, J. Power Sources 178 (2008) 801.
[18] K. Dokko, K. Shiraishi, K. Kanamura, J. Electrochem. Soc. 152 (2005) A2199.
[19] J. Chen, M.J. Vacchio, S. Wang, N. Chernova, P. Zavajil, M.S. Whittingham, Solid State Ionics 178 (2008) 1676.
[20] M.M. Doeff, Y. Hu, F. McLarnon, R. Kostecki, Electrochem. Solid State Lett. 6 (2003) A207.
[21] C.M. Julien, K. Zaghib, A. Mauger, M. Massot, A. Ait-Slah, M. Selmane, F. Gendron, J. Appl. Phys. 100 (2006) 63511.
[22] M. Massot, K. Zaghib, A. Mauger, F. Gendron, C.M. Julien, MRS Proceed. 972 (2006) 0972-AA13-07.
[23] G. Nuspl, C. Vogler, M. Eisgruber, L. Wimmer, N. Schall, C. Fietzek, W. Weydanz, 12th Int. Meet. Lithium Batteries 12 (2004) 293.
[24] G. Nuspl, L. Wimmer, M. Eisgruber, Can. Patent Appl. (2005) CA2537278.
[25] M.L. Trudeau, D. Laul, R. Veillette, A.M. Serventi, K. Zaghib, A. Mauger, C.M. Julien, J. Power Sources 196 (2011) 7383.
[26] P. Axmann, C. Stinner, M. Wohlfahrt-Mehrens, A. Mauger, F. Gendron, A. Mauger, Chem. Mater. 21 (2009) 1936.
[27] A. Franzolet, Bull. Soc. Fr. Minéral. Cristallogr. 100 (1977) 198.
[28] C. Delacourt, J. Rodriguez-Carjaval, B. Schmitt, J.M. Tarascon, C. Masquelier, Solid State Sci. 7 (2005) 1506.
[29] V.A. Streltsov, E.L. Belokoneva, V.G. Tsirelson, N.K. Hansen, Acta Crystallogr. B49 (1993) 147.
[30] N. Amdouni, K. Zaghib, F. Gendron, C.M. Julien, Ionics 12 (2006) 117.
[31] M.T. Paques-Ledent, P. Tarte, Spectrochim. Acta A30 (1974) 673.
[32] C.M. Burma, R. Frech, J. Electrochem. Soc. 151 (2004) 1032.
[33] C.M. Julien, A. Mauger, A. Ait-Salah, M. Massot, F. Gendron, K. Zaghib, Ionics 13 (2007) 395.
[34] N. Ravet, M. Gauthier, K. Zaghib, A. Mauger, J. Goodenough, F. Gendron, C. Julien, Chem. Mater. 19 (2007) 2595.
[35] R. Santoro, R.E. Newnham, Acta Crystallogr. 22 (1967) 344.
[36] K. Zaghib, A. Mauger, J. Goodenough, F. Gendron, C. Julien, Chem. Mater. 19 (2007) 3740.